Geophysical Research Letters

RESEARCH LETTER
10.1029/2022GL098825

Key Points:

- We challenge the traditional perspective that deep Labrador Sea decadal ventilation is mainly achieved by local time-varying deep convection
- Deep decadal variability also arises through mean convective vertical redistribution of upper ocean anomalies entering the Labrador Sea
- We reconstruct the observed Labrador Sea decadal variability using indices for the two mechanisms in a simple multiple regression model

Supporting Information:

Supporting Information may be found in the online version of this article.

Correspondence to:

M. D. Thomas,
Matthew.Thomas@noaa.gov

Citation:

Thomas, M. D., & Zhang, R. (2022). Two sources of deep decadal variability in the central Labrador Sea open-ocean convection region. *Geophysical Research Letters*, *49*, e2022GL098825. https://doi.org/10.1029/2022GL098825

Received 22 MAR 2022
Accepted 27 MAY 2022

Two Sources of Deep Decadal Variability in the Central Labrador Sea Open-Ocean Convection Region

M. D. Thomas[1,2] and R. Zhang[1]

[1]National Oceanic and Atmospheric Administration, Oceanic and Atmospheric Research, Geophysical Fluid Dynamics Laboratory, Princeton, NJ, USA, [2]University Corporation for Atmospheric Research, Boulder, CO, USA

Abstract The ventilation of the central Labrador Sea is important for the uptake of ocean tracers and carbon. Using historical ocean observations, we construct a simple multiple linear regression model that successfully reconstructs the decadal variability of the upper ∼2,000 m of the central Labrador Sea water properties based on observed indices that represent two different open-ocean ventilation mechanisms. The first mechanism is the modification of deep ocean properties through local decadal variability of the Labrador Sea deep convective mixing. The second, more novel, mechanism is the climatological convective vertical redistribution of upper central Labrador Sea temperature and salinity anomalies associated with the nonlocal large-scale subpolar Atlantic Multidecadal Variability and the Atlantic Meridional Overturning Circulation. The ventilated decadal central Labrador Sea signal subsequently spreads into the western subpolar North Atlantic. The results have important implications for predicting decadal ventilated signals in the Labrador Sea that are associated with the large-scale climate variability.

Plain Language Summary The central Labrador Sea is a globally-important region for the modification of deep temperature and salinity. However, the nature of the ventilation mechanisms of the central Labrador Sea is not well understood. The conventional perspective is that time-varying convective mixing in the central Labrador Sea actively modifies deep properties by mediating exchange with the atmosphere. Here using historical ocean observations, we show that in addition to this mechanism the Labrador Sea open-ocean deep convection also acts to vertically redistribute large-scale upper ocean anomalies that can originate outside of the central Labrador Sea and that are associated to variations in the Atlantic Multidecadal Variability, the dominant mode of basin-wide low frequency temperature and salinity fluctuations. Using a simple multiple linear regression model, which combines predictors for the two mechanisms that affect deep central Labrador Sea properties, we demonstrate that we can closely reconstruct the observed decadal variability of the upper ∼2,000 m of the central Labrador Sea temperature, salinity and density. The results will help with the development of decadal prediction systems by improving our understanding of the mechanisms leading to decadal variability in the deep ocean.

1. Introduction

The North Atlantic is an important source region for the ventilation of the deep water properties of the global ocean (e.g., Gebbie & Huybers, 2011; Johnson, 2008), and accordingly also for the deep injection of tracers (Fröb et al., 2016). The mechanisms through which surface properties are ventilated into the deep ocean are still debated, however. While basin-scale and multidecadal-scale fluctuations in the properties of the upper ∼700 m of the suboplar gyre are well described by the Atlantic Multidecadal Variability (AMV; Zhang, 2008; Polyakov et al., 2010; McCarthy et al., 2015; Frajka-Williams et al., 2017; Desbruyères et al., 2020) and its associated mechanisms (Zhang et al., 2019), the origin of deeper subpolar variability is not yet clear, and various theories exist on the mechanisms of deep ventilation. Reconciling these perspectives is important for improving model representation and predictability of the deep ocean (Kieke & Yashayaev, 2015), and for our understanding of how biogeochemical variables such as CO_2 and nutrients are sequestered (Fröb et al., 2016; Hill et al., 2004).

The central Labrador Sea is considered a primary location of deep ventilation. This has commonly been thought to occur through variability in open-ocean deep convection strength, particularly in terms of how it enables time-varying changes in ocean column-integrated buoyancy exchange with the atmosphere (Kieke & Yashayaev, 2015; van Aken et al., 2011; Yashayaev & Loder, 2016). Yet, observational analyses show that the strength of Labrador Sea deep convective ventilation varies at decadal timescales, whereas deep temperature and salinity

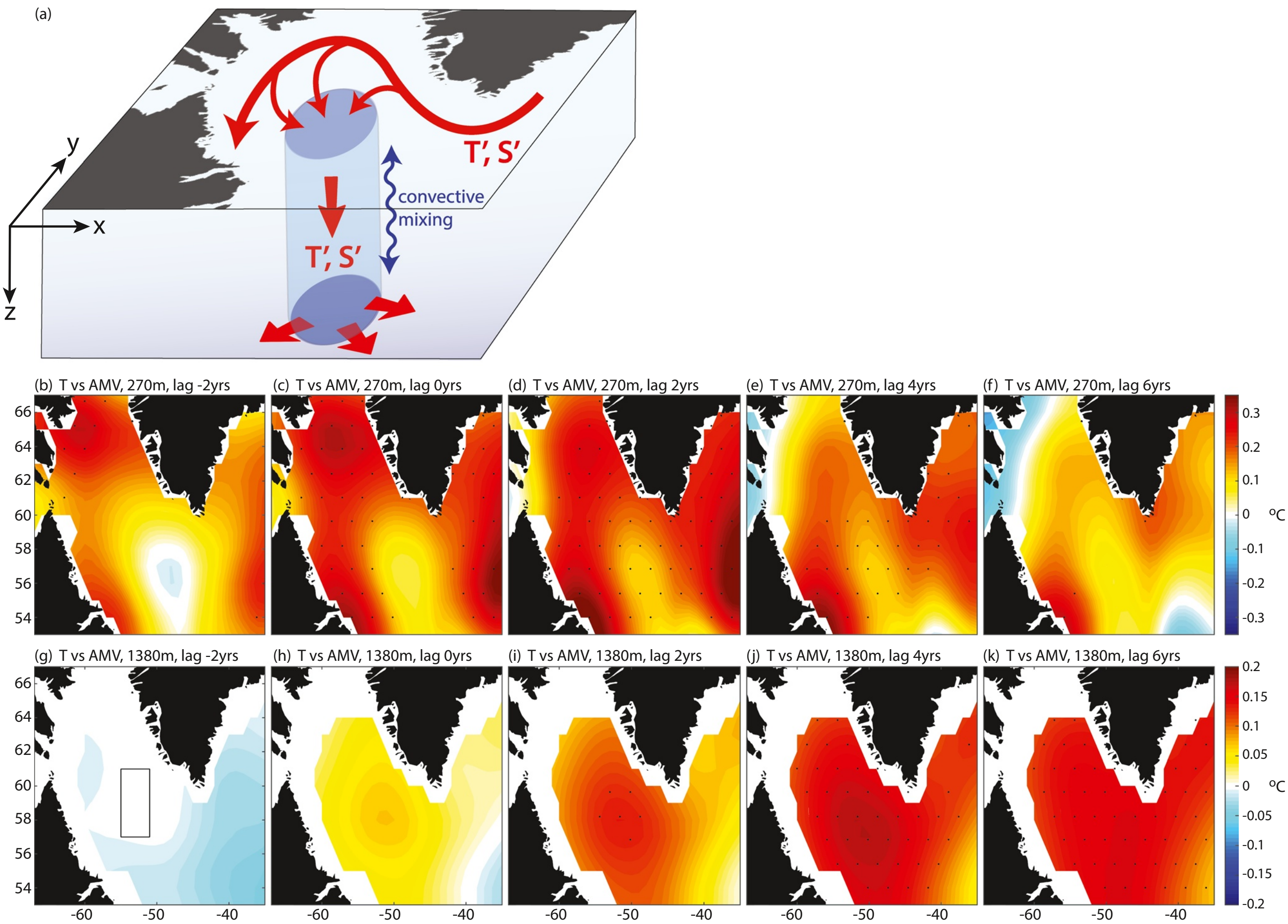

Figure 1. (a) Schematic of the "downward convective redistribution" mechanism over the central Labrador Sea. Maps of the EN4 (b–f) 270 m and (g–k) 1380 m decadal North-West Atlantic subpolar temperatures regressed onto the subpolar Atlantic Multidecadal Variability (AMV) index, at lags increasing from −2 to 6 years. Regressions are normalized per unit standard deviation of the subpolar AMV index (Units °C), and stippling represents significance at 95%.

vary at multidecadal timescales (van Aken et al., 2011). Such multidecadal property anomalies averaged over the western subpolar North Atlantic, and over 700-to-2500 m depth, lag the mutually-coherent near-surface low-frequency anomalies by about 5 years (Hodson et al., 2014), indicating downward propagation. Furthermore, since the subpolar upper ocean temperature and salinity anomalies are strongly coherent with each other, which only occurs at decadal and longer timescales and is a key element of the observed AMV, these anomalies likely associate with the large-scale subpolar circulation and the Atlantic Meridional Overturning Circulation (AMOC) (Yan et al., 2019; Zhang, 2017; Zhang et al., 2019). This vertical redistribution of larger-scale variability would likely stand as a distinct ventilation mechanism from that induced by variability in open-ocean deep convection strength. Recently, it has been suggested that the mechanism of downward propagation of upper subpolar AMV-related temperature anomalies through boundary vertical advection and diffusion is the dominant origin of deep temperature variability in the subpolar gyre (Desbruyères et al., 2020). Here, we instead focus on the central Labrador Sea region to understand the role of open-ocean deep convection in the vertical redistribution of upper ocean AMV-related anomalies of both temperature and salinity in the central Labrador Sea, as described in Figure 1a, and determine its relative importance compared to deep convective variability.

In this study, we use historical observations to assess the two different roles of convective vertical mixing in the deep properties of the central Labrador Sea, where mixed layers (Holte et al., 2017) and low Potential Vorticity (PV) (Li et al., 2019; van Aken et al., 2011) are deepest. We construct a simple multiple linear regression model for the decadal ventilation of the central Labrador Sea temperature and salinity, which demonstrates that both

10.1029/2022GL098825

the time-varying convective vertical mixing strength and also the climatological downward convective mixing of upper ocean anomalies are important.

2. Data and Methods

2.1. Data

To investigate the central Labrador Sea ventilation mechanisms and to construct the multiple linear regression model of decadal variability, we use the following observational data: the UK Met Office EN4.2.1 (henceforth EN4) gridded ocean temperature and salinity data set (Good et al., 2013) covering all depths, from years 1951 to 2019; oxygen concentration at 1500 m in the central Labrador Sea from years 1951 to 2017 (compiled from the van Aken et al. (2011) and Rhein et al. (2017) data; we refer readers to these papers and to the supplementary section for further details); and the Hadley Center Sea Ice and Sea Surface Temperature (HadISST) data set (Rayner et al., 2003) from years 1951 to 2019. Due to the sparseness of early historical ocean observations we test the robustness of some conclusions derived from EN4 by applying repeat analyses to the Ishii et al. (2006) gridded data set of temperature and salinity (henceforth Ishii data set). This covers depths down to 1,500 m and years 1951–2012. Unless otherwise stated, all annual mean data used in this manuscript are 10 years low-pass filtered, and nonlinearly detrended. See the Supporting Information S1 extended data description for more information.

2.2. A Multiple Linear Regression Model of the Central Labrador Sea Decadal Ventilation

We construct a simple multiple linear regression model for the Labrador Sea deep variability based on two observed indices that represent two different ventilation mechanisms. The first mechanism is the modification of deep-water properties through decadal variability in deep convection strength, which can modify the rate of vertical mixing and mediate fluxes between the deep ocean and the atmosphere. The second mechanism is the climatological convective vertical redistribution of upper-ocean temperature and salinity anomalies, with decadal variability that can originate outside of the Labrador Sea. Since these two mechanisms are not fully independent (discussed further below), we use a multiple regression method that can also account for the inter-correlation between the two predictors. We henceforth refer to the two mechanisms as "time-varying convective ventilation" and "downward convective redistribution of upper ocean anomalies", for which we respectively construct observed indices as follows:

1. The observed oxygen concentration at 1500 m (O_2^{1500m}) in the central Labrador Sea (the domain shown by the black box in Figure 1) (Figure 3b). It depends primarily on the downward time-varying mixing of near-surface waters, and is a good indicator of deep convection strength since winter near-surface concentrations remain relatively constant in time (e.g., Rhein et al., 2017; van Aken et al., 2011; Yashayaev & Loder, 2016). Above the permanent thermocline at 1500m its concentration reflects deeper convective events (as compared to the summer thermocline depth of 100 m; Holte et al., 2017). This oxygen index is strongly anti-correlated with the central Labrador Sea PV at the same level over the past several decades (van Aken et al., 2011), suggesting that it is a reliable indicator for the time-varying Labrador Sea deep convection. Oxygen concentration also does not rely on calculations of vertical density gradients, which can amplify noise in patchy historical data. There is no significant trend in O_2^{1500m} over the period 1951–2017 (see SI for significance testing).
2. The observed temperature and salinity at 270 m depth and averaged over the central Labrador Sea (black box in Figure 1), henceforth T^{270m} and S^{270m} respectively (Figure 3a). T^{270m} and S^{270m} (In the absence of a strong correlation to O_2^{1500m}) can be used as indicators of the near-surface anomalies that can be redistributed downward below the base of the summer thermocline. Any positive covariance of the 270 m indices with the deeper properties would indicate that both positive and negative anomalies are mixed downward. These near-surface anomalies exhibit multidecadal variability that differs from the convective variability, and are associated with the large-scale AMV signal that can be generated remotely outside of the Labrador Sea region.

Use of the 270 m properties is preferable to the properties at the surface, where seasonal stratification and atmospheric damping are stronger and where freshening events like the great salinity anomaly (Dickson et al., 1988) can affect the surface stratification to create isolated surface temperature and salinity anomalies. While simply defined, we also assume it to represent the region below the summer thermocline from where properties are ventilated into the permanent thermocline.

Using O_2^{1500m} and the subsurface properties (T^{270m} and S^{270m}) as predictors, we construct a multiple linear regression model (Zhang, 2015) of central Labrador Sea temperature and salinity at all depths according to

$$T(z,t) = -\alpha_T(z)O_2^{1500m}(t-\tau_T(z)) + \beta_T(z)T^{270m}(t-\lambda_T(z)) + \epsilon_T(z), \quad (1)$$

$$S(z,t) = -\alpha_S(z)O_2^{1500m}(t-\tau_S(z)) + \beta_S(z)S^{270m}(t-\lambda_S(z)) + \epsilon_S(z), \quad (2)$$

where T and S are the time- and depth-dependent reconstructed central Labrador Sea temperature and salinity, α and β are the depth-dependent regression coefficients for the time-dependent 1500m oxygen (O_2^{1500m}) and subsurface property predictors (T^{270m}, S^{270m}), and ϵ_T and ϵ_S are the corresponding noise, respectively. τ and λ represent depth-dependent temporal lag offsets between the predictor and reconstructed variables, which are restricted to non-negative values so that the predictors either lead or are in-phase with the reconstructed variables. Subscripts T and S denote whether application is to the temperature or salinity regression models, respectively. Since the two mechanisms act on temperature and salinity variability, and not directly on water density, the depth-dependent reconstruction for Labrador Sea density, σ_2, is calculated from the reconstructed T and S according to the equation of state for seawater.

The two predictors are not fully independent, since variable convective mixing can affect subsurface temperatures and salinities, and vice versa through pre-conditioning for convection (Oltmanns et al., 2018; Straneo et al., 2003). However, in addition to locally generated variability, the 270 m properties can also exhibit variability that originates from outside of the Labrador Sea. Accordingly, we find that O_2^{1500m} lag-correlates with T^{270m} at −0.51 at 4 years lag (i.e., with temperatures lagging O_2^{1500m}) that is not significant at 95%, and with S^{270m} at −0.57 at −7 years lag (salinities leading O_2^{1500m}) that is significant at 95% (see SI for significance testing). The negative lag between convective variability and S^{270m} suggests a possible pre-conditioning timescale for the time-varying convection, while the positive lag of the relationship with T^{270m} may just be due to noise in this non-significant correlation. The effect of these inter-correlations between predictors is accounted for by the regression coefficients in the multiple regression model, and does not hinder its usage.

Finally, to study the linkage of the subpolar properties with the large-scale signal, we calculate the subpolar AMV index as the subpolar-average (from 50°N to 65°N) of residual HadISST Sea Surface Temperature (SST) anomalies. The residual SST is the SST anomaly with the globally-averaged SST anomaly removed by regressing at each location (Zhang et al., 2019). We also derive the observed timeseries of the so-called AMOC fingerprint in EN4 (T_{sub}; Zhang, 2008), a previously identified proxy for the multidecadal AMOC variability, that is defined as the leading Empirical Orthogonal Function (EOF) mode of detrended 400 m temperature anomalies in the North Atlantic from 30 to 65°N and 0–80°W.

3. Results

3.1. Decadal Ventilation in the Central Labrador Sea

We demonstrate that the central Labrador Sea acts as the principle ventilation chimney of decadal anomalies, first by lag-regressing the observed 270 and 1380 m temperatures with the subpolar AMV index (Figure 1; Figures S1a–S1j in Supporting Information S1) and AMOC fingerprint (Figures S1k–S1t in Supporting Information S1). The 270 m temperature anomalies associated with the AMV develop in the northern subpolar gyre, peaking at zero lag before then weakening (see also Drews & Greatbatch, 2017). The development of this signal is spread over the boundary regions of the subpolar gyre, and mixed into the upper central Labrador Sea through lateral eddy mixing occurring throughout the upper ocean here (Bracco et al., 2008; Pennelly & Myers, 2022; Tagklis et al., 2020). The deep temperature signal subsequently develops in the deep convective region of the Labrador Sea, before then laterally spreading. Although historical data are geographically sparse, possibly biasing statistical signatures, the deep anomaly patterns are consistent with the vertical convective redistribution mechanism that occurs in the Labrador Sea deep convection site (Figure 1a). Since net vertical advection is small in convection patches (Send & Marshall, 1995), and vertical mixing is high (of 1 $m^2\ s^{-1}$ or higher; Marshall & Schott, 1999), the results suggest that the vertical redistribution of these external anomalies inside the central Labrador Sea is achieved through deep-convective mixing.

Similar spatial spreading patterns are found for salinity anomalies lag-regressed onto the subpolar AMV index (Figures S2a–S2j in Supporting Information S1). And lag-regressions of the subsurface and deep

10.1029/2022GL098825

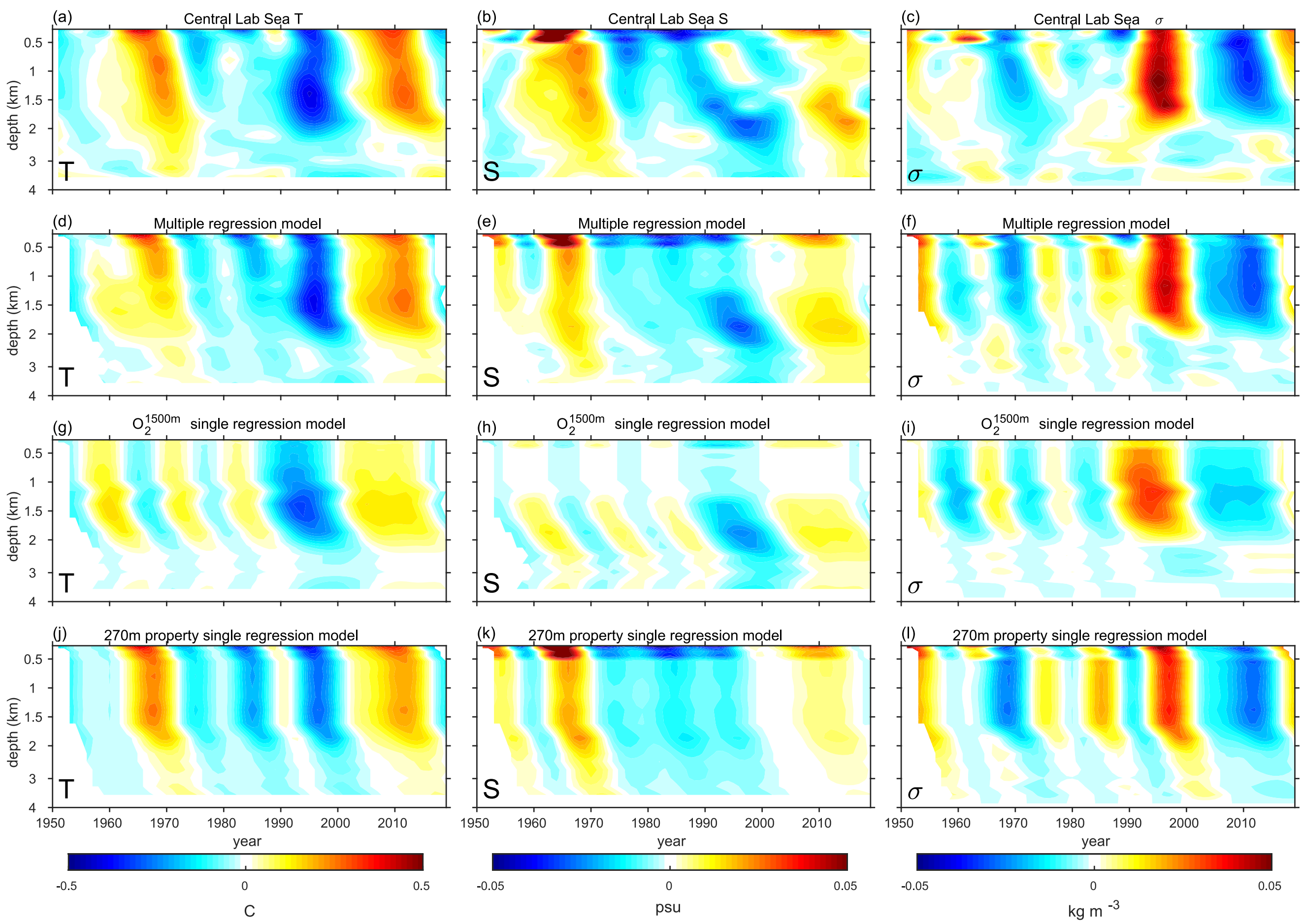

Figure 2. Depth versus time Hovmöller diagram for the area-averaged central Labrador Sea anomalies of (a, d, g, and j) temperature (°C), (b, e, h, and k) salinity (psu), (c, f, i, and l) density (σ_2; kg m^{-3}). (a–c) Observations, and their reconstructions based on the (d–f) multiple linear regression models, (g–i) the O_2^{1500m}-based linear regression models and (j–l) the 270 m property-based linear regression models.

temperature/salinity anomalies on the observed AMOC fingerprint also exhibit similar results (Figures S1k–S1t and S2k–S2t in Supporting Information S1), suggesting that coherent deep central Labrador Sea temperature and salinity anomalies lag the AMV and AMOC, not the other way around as has traditionally been assumed. Finally, anomalies spread eastward in a pattern that is consistent with the observed pathways of Labrador Sea water (Bower et al., 2009; Lavender et al., 2000; Zou & Lozier, 2016) (Figures S1, S2, and S3 in Supporting Information S1). Similar to the spreading pattern of the AMV signature, the central Labrador Sea temperature and salinity anomalies at 1870 m that are associated with time-varying Labrador Sea deep convection also spread into the deep North Atlantic (Figure S3 in Supporting Information S1). While the Nordic Seas are also important for ventilation of deep waters (Gebbie & Huybers, 2011), they are less important for the decadal to multidecadal signal here. And although the Labrador Sea open-ocean deep convection makes a relatively weak contribution to the AMOC strength (Lozier et al., 2019; Pickart and Spall, 2007; Zhang and Thomas, 2021), it is important for ventilation.

To determine the vertical coherence and track the downward propagation of ventilated anomalies, Figures 2a–2c shows depth-time Hovmöller diagrams of the detrended temperature, salinity and density anomalies averaged over the central Labrador Sea (black box in Figure 1f). It is first worth noting that, unlike earlier estimates using shorter timeseries data (Curry et al., 2003; Levitus et al., 2000), the EN4 and Ishii Labrador Sea properties exhibit only small trends that are not significant over this timeframe at any depth (not shown). This is consistent with Zanna et al. (2019) who show that the observed ocean heat uptake over the historical period has occurred primarily in the Southern Ocean and mid-latitudes.

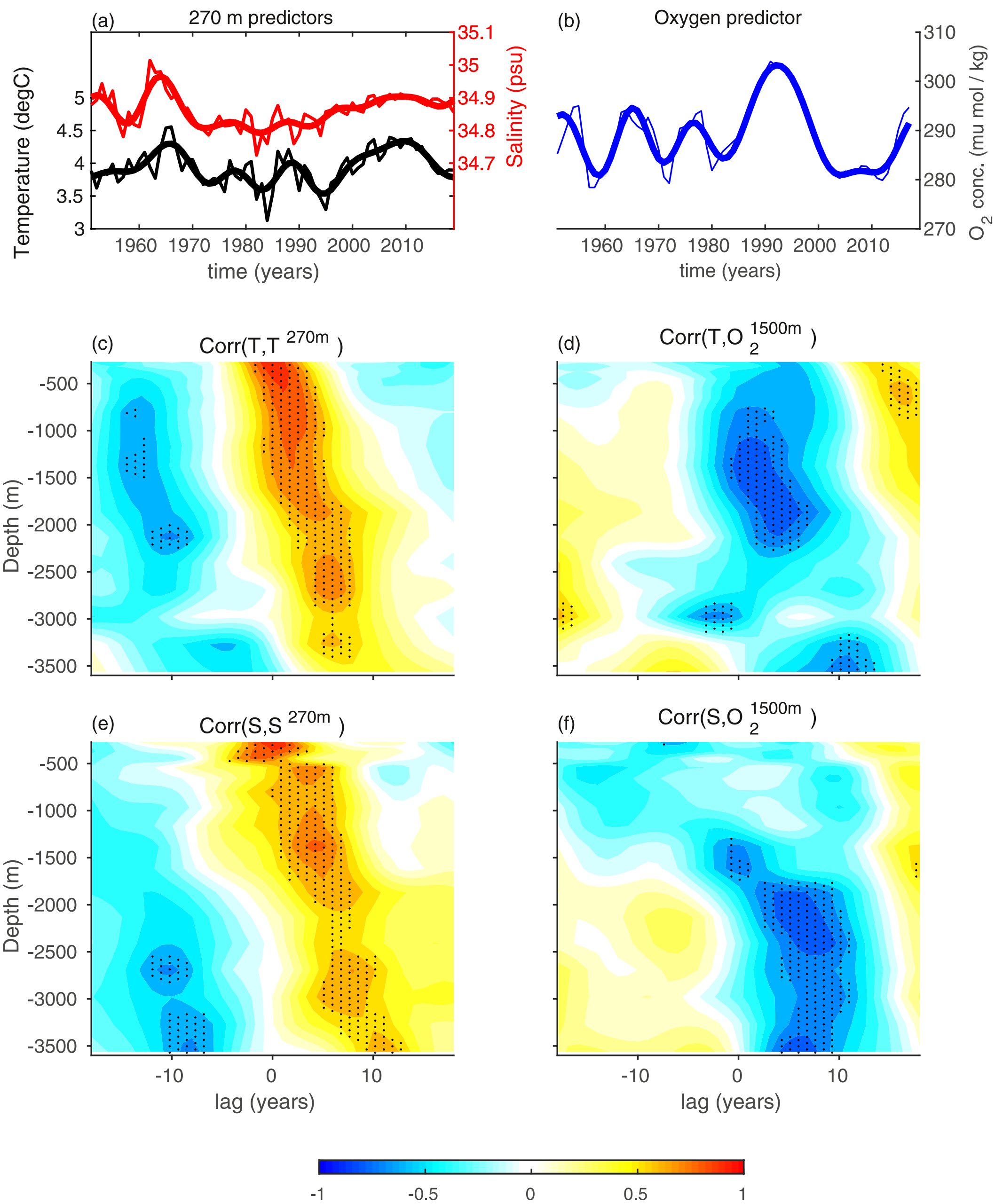

Figure 3. Timeseries of the (a) 270 m and (b) O_2^{1500m} predictors. Lag correlation of the (c,d) temperature and (e,f) salinity at each depth between (c) T^{270m}, (e) S^{270m}, and (d,f) O_2^{1500m}. Stippling represents 95% significance.

The detrended Labrador Sea property anomalies undergo strong decadal to multidecadal variability (e.g., Hodson et al., 2014; Yashayaev & Loder, 2016). This is true for anomalies of both polarities, and not just the cold events that are often the focus (Figures 2a–2c). Before application of the multiple linear regression, it is helpful to determine the relationship of central Labrador Sea properties to each ventilation process. In Figure 3 we lag correlate the properties, at every depth, with the two predictors, 1500 m O_2 (for convective variability) and the 270 m properties, T^{270m} and S^{270m} (for convective redistribution). The temperatures are positively correlated to T^{270m} at all depths, with lag time increasing with depth (Figure 3c), indicating that both positive and negative upper temperature anomalies are redistributed downward. The signal between ∼500 m and ∼1500 m has near-constant phase and amplitude (Figures 2j–2l), with a vertical propagation timescale that is too short to be accounted for by the roughly 150 m/yr vertical velocities found in the Labrador boundary current (Liang et al., 2017). Similarly, the near-constant phase and amplitude cannot be explained by an effective vertical diffusivity of 3×10^{-3} m^2 s^{-1}, intended to account for all boundary mixing processes (including eddies) (Desbruyères et al., 2020), which would take approximately a decade to mix anomalies across this 1000 m distance and would depreciate the signal with depth. The fast propagation over this depth range is instead consistent with the high mixing rate within the low-PV central Labrador Sea deep convection region, where mixing coefficients can exceed 1 m^2 s^{-1} (Marshall & Schott, 1999). Over this region, the PV/stratification is low from 500 to 1500 m, and relatively higher above and below this depth range (van Aken et al., 2011). Hence above 500 m and below 1500 m, the vertical mixing is relatively weaker, requiring longer timescales to mix across the depth ranges 270–500 m (∼2 years) and 1,500 m–2,000 m (∼3 years). At deeper depths, the reach of climatological convective mixing diminishes leading to longer lag times, possibly as other processes become important.

The effects of the redistribution mechanism weaken with depth (Figures 3c and 3e) as convective variability becomes increasingly important (Figures 3d and 3f). Negative correlations between temperature and O_2^{1500m} are found at all depths (Figure 3d), indicating that there is also column heat loss to the atmosphere (e.g., Yashayaev & Loder, 2016), peaking at ∼1600 m as the effects of the downward redistribution mechanism diminish. Correlations then weaken again below the permanent thermocline where colder temperatures are less sensitive to heat loss. As noted by Rhein et al. (2017), while O_2 saturation is a function of temperature, an upper bound of only 4 μmol kg^{-1} change in O_2 solubility equilibrium is associated with a 0.5°C decadal temperature change at the Labrador Sea Water layer. This is relatively small compared to the range of O_2^{1500m} decadal variability over this temperature range (Figure 3b).

The ventilation predictors share similar general relationships with the salinities as the temperatures, with a positive correlation to S^{270m} in the upper ocean (Figure 3e) giving way to a stronger negative correlation to O_2^{1500m} at depth (Figure 3f). A negative correlation to O_2^{1500m} at all depths suggests that during stronger convection decades, a column salinity reduction or storage of freshwater occurs over the Labrador Sea convection region that is likely associated with enhanced atmospheric freshwater forcing and/or enhanced lateral oceanic freshwater transport convergence. This salinity correlation is most apparent below ∼1.7 km depth where the background salinity is higher and more sensitive to changes in convective mixing strength. That is, the salinity contrast between periods of strong and weak deep convection below 1.7 km depth is larger than that above 1.7 km depth (e.g., Yashayaev & Loder, 2016), and thus less affected by noise. The longer lag times found at these depths also indicates that mechanisms beyond the local convective mixing may become important here, such as the influence of the overflow water, horizontal exchange with water in the boundary and Irminger Sea, or vertical diffusion.

Similar lag-correlation analyses applied to the Ishii et al. (2006) temperature and salinity data produces qualitatively similar results to those from EN4 (Figure S4 in Supporting Information S1), lending support to the robustness of the datasets and findings.

3.2. Labrador Sea Properties Reconstructed by the Multiple Regression Model

The differing relationships of the central Labrador Sea properties with the two ventilation mechanisms indicate the possibility of constructing a multiple linear regression model based only on the two ventilation indices. Using Equations 1 and 2 we reconstruct timeseries of central Labrador Sea temperature and salinity separately at each depth level, with lag times λ and τ chosen according to the depth-dependent lags of maximum correlation identified in Figure 3. Since we expect each mechanism to impact T and S in a similar manner (even if the respective magnitudes of these impacts differ), lag times are selected so that $\lambda_T = \lambda_S$ and $\tau_T = \tau_S$ at each depth level. Our main conclusions are not affected, however, if lag timescales are allowed to vary independently for T and S. λ is set equal to the lag of maximum positive correlation between T^{270m} and T at each depth: this is because the salinity correlations are noisier and, as described below, the Ishii et al. (2006) Labrador Sea salinities are less noisy with more similarity to temperature, thereby indicating that the EN4 salinity noise could be unrealistic. τ is chosen according to: the lags of significant negative correlation between T and O_2^{1500m} over the 1000–2000 m depth range; the lags of significant correlation between S and O_2^{1500m} below 2000 m; and tau = 0 years above 1000 m where correlations are not significant. We note some data set dependence in τ_T, which at 1500 m depth is 2 years in EN4 while in the Ishii data it is closer to 1 year (Figure S4 in Supporting Information S1).

Figures 2d and 2e shows the multiple regression model reconstructions of the central Labrador Sea T and S, and Figure 2f shows reconstructed σ_2 calculated from the T and S reconstructions. For comparison, the single

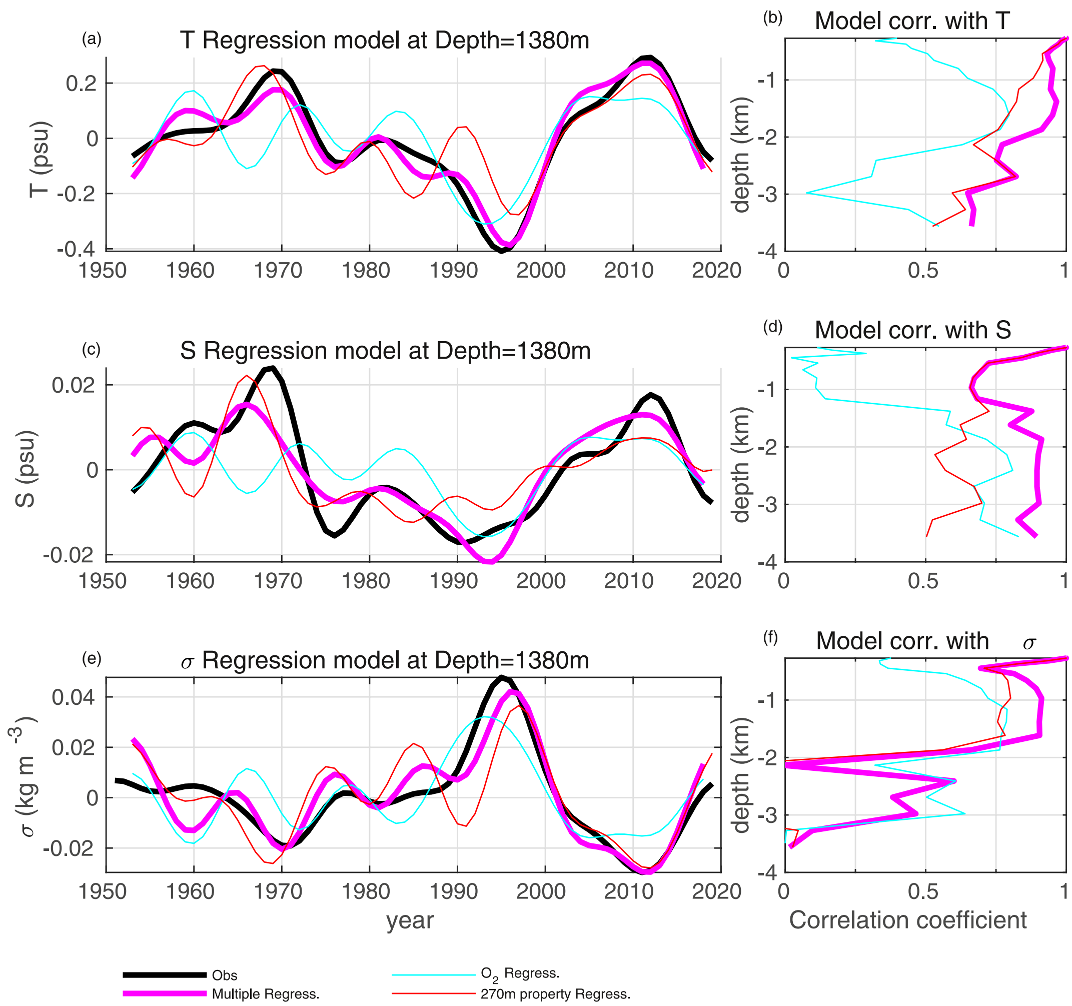

Figure 4. (a,b) Temperature, (c,d) salinity and (e,f) density (a,c,e) timeseries for the (thick black line) original, (thick magenta line) multiple linear and (thin lines) single-variable regression models (colored lines; see legend) at 1,380 m, and (b,d,f) correlation coefficients at each depth between the regression models and the original timeseries (using the same legend). All multiple linear regression model correlation coefficients that exceed ∼0.75 in each case are significant at 95%.

variable linear regression model reconstructions are also calculated using each of the two predictors separately (Figures 2g–2l). In the top ∼2000 m, the multiple regression model reconstructed T consistently achieves coefficients exceeding 0.9 (∼0.97 at 1380 m depth) when correlated with the observed data (Figure 4b). Since the 270 m anomalies are related to the remote basin-scale anomalies described by the subpolar AMV (Figure 1), if we use the subpolar AMV index instead of T_{270m} as the multiple regression predictor then the reconstruction is also reasonable but the peak correlation with the observed data is reduced from ∼0.97 to ∼0.85.

The skill of the multiple regression model reconstructions can be compared to the two single-variable regression reconstructions, which capture the shifting relative importance of the two predictors with depth (Figure 4). The anomalies reconstructed by each of the two individual ventilation mechanisms exhibit comparable amplitudes and they counter or reinforce each other during different periods (Figures 2 and 4). Only by accounting for both ventilation mechanisms in the multiple regression model do we achieve the best comparison with observations (Figures 2 and 4). Due to correlation between the two predictors, the sum of the two single regression models includes a redundant inter-correlated term. This term can be diagnosed as the difference between the multiple regression reconstruction (without the redundant term) and the sum of the two single regression reconstructions, which typically has a magnitude of only ∼15% of the multiple regression reconstruction.

For salinity reconstructions, in the approximate depth range of 500–1100 m, the correlations between multiple regression reconstructed and observed salinity anomalies are typically only approximately 0.66–0.7 due to a weaker relationship with S^{270m}. It isn't clear if this is because historical salinity data is noisier than temperature data. However, while similar general results are obtained using the Ishii et al. (2006) data, its salinity data is less noisy and allows a better reconstruction (Figure S5 in Supporting Information S1). The EN4 salinity reconstructions then increase in accuracy toward deeper depths (~0.91 at 1868 m depth) due to the stronger relationship with O_2^{1500m} (Figure 3f), as described earlier.

The multiple regression reconstructed density timeseries achieves correlations with observations that typically exceed 0.85 in the depth-range ~500–1600 m (peaking at 0.91; Figure 4). This is despite the relatively poor salinity reconstruction at these depths. The conclusions from the multiple regression model are not sensitive to the chosen size of the central Labrador Sea domain (black box in Figure 1g). However, if the box is enlarged to encompass the whole Labrador Sea region then the multiple regression model correlations are slightly worsened.

4. Conclusion and Discussion

In this study, using historical observations, we constructed a simple and novel multiple linear regression model, which successfully reconstructs the evolution of the upper ~2,000 m of the central Labrador Sea water properties (Figures 2 and 4). Applied separately to temperature and salinity, the multiple regression model uses only two observed predictors, the anomalous oxygen concentration at 1500 m depth and the property anomaly at 270 m in the central Labrador Sea, to represent two different ventilation mechanisms over the open-ocean deep convection region. The first mechanism, which modifies ocean column properties through decadal variability of deep convective mixing, is well known. The second mechanism is more novel, and is the vertical redistribution of coherent multidecadal near-surface property anomalies (associated with the observed subpolar AMV index and the AMOC) into the deep ocean via central Labrador Sea convective mixing, where low vertical stratification and PV are found. As such, the central Labrador Sea region acts as an important ventilation chimney to the deep ocean through two important processes of open-ocean deep convection: the contribution due to the time-varying deep convection and the contribution from the climatological downward convective redistribution of upper ocean anomalies. While both are related to convective mixing, and they impact on each other through mutual (and time-dependent) conditioning of the water column and its convective stability, the two mechanisms lead to distinct ventilated variability. Only by accounting for both ventilation mechanisms do we achieve the best reconstructions of observations, in contrast to many previous studies that only considered the convective variability as important. The salinity and temperature reconstructions can subsequently be used to successfully reconstruct density variability.

The temperature and salinity anomalies in most regions in the deep western subpolar North Atlantic lag the observed subpolar AMV and AMOC indices (Figure 1; Figure S2 in Supporting Information S1), since it takes some years for signals to translate into the deep ocean and then radially spread. These propagation timescales between the near-surface Labrador Sea and the deep subpolar North Atlantic (Figures 1 and 2) therefore bring the results into consistency with earlier studies that show the multidecadal variability of the upper and deeper subpolar gyre are opposed over much of the region when calculated at zero lag (Kim et al., 2018; Polyakov et al., 2010). Similar results to those studies can be reproduced using the EN4 data (not shown).

The results of this study have important implications for understanding and predicting the decadal ventilated signal in the central Labrador Sea that is associated with the large-scale climate variability. Both ventilation mechanisms are important sources of deep variability that counter or reinforce each other during different periods, and this knowledge will help guide efforts in creating prediction models of the central Labrador Sea. Many climate models do not accurately represent Labrador Sea deep convection (Roberts et al., 2020) and its associated ventilation mechanisms, and improving its representation in models will be important both for better decadal-mutidecadal prediction as well as for gaining a better understanding of the processes and interactions involved. Our simple approach of combining two ventilation mechanisms might also be revised and expanded to understand and predict the ventilation of other tracers spread from the central Labrador Sea into the deep subpolar North Atlantic.

Data Availability Statement

Observational data used in this study can be accessed at the following sources: EN4 and HadISST can be accessed at the Met Office webservers at https://www.metoffice.gov.uk/hadobs/en4/ and https://www.metoffice.gov.uk/hadobs/hadisst/, respectively; the Ishii data set from https://doi.org/10.5065/Y6CR-KW66; and oxygen concentration data from van Aken et al. (2011, https://doi.org/10.1016/j.dsr.2011.02.008) and Rhein et al. (2017, https://doi.org/10.1098/rsta.2016.0321).

Acknowledgments

This research from the Geophysical Fluid Dynamics Laboratory (GFDL) is supported by NOAA's Science Collaboration Program and administered by UCAR's Cooperative Programs for the Advancement of Earth System Science (CPAESS) under award #NA21OAR4310383, and the GFDL base funding. We acknowledge GFDL resources made available for this research. We are grateful to Graeme MacGilchrist and Brandon Reichl for helpful comments on the manuscript, Marion Alberty for useful discussions, GFDL operations for computational support, Catherine Raphael for illustration support, and two anonymous reviewers for their constructive feedback.

References

Bower, A. S., Lozier, M. S., Gary, S. F., & Böning, C. W. (2009). Interior pathways of the north Atlantic meridional overturning circulation. *Nature*, *459*(7244), 243–242. https://doi.org/10.1038/nature07979

Bracco, A., Pedlosky, J., & Pickart, R. S. (2008). Eddy formation near the west coast of Greenland. *Journal of Physical Oceanography*, *38*(9), 1992–2002. https://doi.org/10.1175/2008jpo3669.1

Curry, R., Dickson, B., & Yashayaev, I. (2003). A change in the freshwater balance of the Atlantic ocean over the past four decades. *Nature*, *426*(6968), 826–829. https://doi.org/10.1038/nature02206

Desbruyères, D. G., Sinha, B., McDonagh, E. L., Josey, S. A., Holliday, N. P., Smeed, D. A., et al. (2020). Importance of boundary processes for heat uptake in the subpolar north Atlantic. *Journal of Geophysical Research: Oceans*, *125*(9), e2020JC016366. https://doi.org/10.1029/2020jc016366

Dickson, R. R., Meincke, J., Malmberg, S.-A., & Lee, A. J. (1988). The "great salinity anomaly" in the northern North Atlantic 1968–1982. *Progress in Oceanography*, *20*(2), 103–151. https://doi.org/10.1016/0079-6611(88)90049-3

Drews, A., & Greatbatch, R. J. (2017). Evolution of the Atlantic multidecadal variability in a model with an improved north Atlantic current. *Journal of Climate*, *30*(14), 5491–5512. https://doi.org/10.1175/jcli-d-16-0790.1

Frajka-Williams, E., Beaulieu, C., & Duchez, A. (2017). Emerging negative Atlantic multidecadal oscillation index in spite of warm subtropics. *Scientific Reports*, *7*(1), 1–8. https://doi.org/10.1038/s41598-017-11046-x

Fröb, F., Olsen, A., Våge, K., Moore, G. W. K., Yashayaev, I., Jeansson, E., & Rajasakaren, B. (2016). Irminger sea deep convection injects oxygen and anthropogenic carbon to the ocean interior. *Nature Communications*, *7*(1), 1–8. https://doi.org/10.1038/ncomms13244

Gebbie, G., & Huybers, P. (2011). How is the ocean filled? *Geophysical Research Letters*, *38*(6), L06604. https://doi.org/10.1029/2011gl046769

Good, S. A., Martin, M. J., & Rayner, N. A. (2013). En4: Quality controlled ocean temperature and salinity profiles and monthly objective analyses with uncertainty estimates. *Journal of Geophysical Research: Oceans*, *118*(12), 6704–6716. https://doi.org/10.1002/2013jc009067

Hill, C., Bugnion, V., Follows, M., & Marshall, J. (2004). Evaluating carbon sequestration efficiency in an ocean circulation model by adjoint sensitivity analysis. *Journal of Geophysical Research*, *109*(C11), 2002JC001598. https://doi.org/10.1029/2002jc001598

Hodson, D. L. R., Robson, J. I., & Sutton, R. T. (2014). An anatomy of the cooling of the North Atlantic Ocean in the 1960s and 1970s. *Journal of Climate*, *27*(21), 8229–8243. https://doi.org/10.1175/jcli-d-14-00301.1

Holte, J., Talley, L. D., Gilson, J., & Roemmich, D. (2017). An argo mixed layer climatology and database. *Geophysical Research Letters*, *44*(11), 5618–5626. https://doi.org/10.1002/2017gl073426

Ishii, M., Kimoto, M., Sakamoto, K., & Iwasaki, S.-I. (2006). Steric sea level changes estimated from historical ocean subsurface temperature and salinity analyses. *Journal of Oceanography*, *62*(2), 155–170. https://doi.org/10.1007/s10872-006-0041-y

Johnson, G. C. (2008). Quantifying Antarctic bottom water and north Atlantic deep water volumes. *Journal of Geophysical Research*, *113*(C5), C05027. https://doi.org/10.1029/2007jc004477

Kieke, D., & Yashayaev, I. (2015). Studies of Labrador Sea water formation and variability in the subpolar north Atlantic in the light of international partnership and collaboration. *Progress in Oceanography*, *132*, 220–232. https://doi.org/10.1016/j.pocean.2014.12.010

Kim, W. M., Yeager, S. G., & Danabasoglu, G. (2018). Key role of internal ocean dynamics in Atlantic multidecadal variability during the last half century. *Geophysical Research Letters*, *45*(24), 13–449. https://doi.org/10.1029/2018gl080474

Lavender, K. L., Davis, R. E., & Owens, W. B. (2000). Mid-depth recirculation observed in the interior Labrador and irminger seas by direct velocity measurements. *Nature*, *407*(6800), 66–69. https://doi.org/10.1038/35024048

Levitus, S., Antonov, J. I., Boyer, T. P., & Stephens, C. (2000). Warming of the world ocean. *Science*, *287*(5461), 2225–2229. https://doi.org/10.1126/science.287.5461.2225

Li, F., Lozier, M. S., Danabasoglu, G., Holliday, N. P., Kwon, Y.-O., Romanou, A., et al. (2019). Local and downstream relationships between Labrador Sea water volume and north Atlantic meridional overturning circulation variability. *Journal of Climate*, *32*(13), 3883–3898. https://doi.org/10.1175/jcli-d-18-0735.1

Liang, X., Spall, M., & Wunsch, C. (2017). Global ocean vertical velocity from a dynamically consistent ocean state estimate. *Journal of Geophysical Research: Oceans*, *122*(10), 8208–8224. https://doi.org/10.1002/2017jc012985

Lozier, M. S., Li, F., Bacon, S., Bahr, F., Bower, A. S., Cunningham, S. A., et al. (2019). A sea change in our view of overturning in the subpolar north Atlantic. *Science*, *363*(6426), 516–521. https://doi.org/10.1126/science.aau6592

Marshall, J., & Schott, F. (1999). Open-ocean convection: Observations, theory, and models. *Reviews of Geophysics*, *37*(1), 1–64. https://doi.org/10.1029/98RG02739

McCarthy, G. D., Haigh, I. D., Hirschi, J. J.-M., Grist, J. P., & Smeed, D. A. (2015). Ocean impact on decadal Atlantic climate variability revealed by sea-level observations. *Nature*, *521*(7553), 508–510. https://doi.org/10.1038/nature14491

Oltmanns, M., Karstensen, J., & Fischer, J. (2018). Increased risk of a shutdown of ocean convection posed by warm north Atlantic summers. *Nature Climate Change*, *8*(4), 300–304. https://doi.org/10.1038/s41558-018-0105-1

Pennelly, C., & Myers, P. G. (2022). Tracking irminger rings' properties using a sub-mesoscale ocean model. *Progress in Oceanography*, *201*, 102735. https://doi.org/10.1016/j.pocean.2021.102735

Pickart, R. S., & Spall, M. A. (2007). Impact of Labrador Sea Convection on the North Atlantic Meridional Overturning Circulation. *Journal of Physical Oceanography*, *37*(9), 2207–2227. https://doi.org/10.1175/jpo3178.1

Polyakov, I. V., Alexeev, V. A., Bhatt, U. S., Polyakova, E. I., & Zhang, X. (2010). North Atlantic warming: Patterns of long-term trend and multidecadal variability. *Climate Dynamics*, *34*(2), 439–457. https://doi.org/10.1007/s00382-009-0589-5

Rayner, N. A., Parker, D. E., Horton, E. B., Folland, C. K., Alexander, L. V., Rowell, D. P., et al. (2003). Global analyses of sea surface temperature, sea ice, and night marine air temperature since the late nineteenth century. *Journal of Geophysical Research: Atmospheres*, *108*(D14), 4407. https://doi.org/10.1029/2002JD002670

Rhein, M., Steinfeldt, R., Kieke, D., Stendardo, I., & Yashayaev, I. (2017). Ventilation variability of Labrador Sea water and its impact on oxygen and anthropogenic carbon: A review. *Philosophical Transactions of the Royal Society A: Mathematical, Physical & Engineering Sciences*, *375*(2102), 20160321. https://doi.org/10.1098/rsta.2016.0321

Roberts, M. J., Jackson, L. C., Roberts, C. D., Meccia, V., Docquier, D., Koenigk, T., et al. (2020). Sensitivity of the Atlantic meridional overturning circulation to model resolution in CMIP6 HighResMIP simulations and implications for future changes. *Journal of Advances in Modeling Earth Systems*, *12*(8), e2019MS002014. https://doi.org/10.1029/2019ms002014

Send, U., & Marshall, J. (1995). Integral effects of deep convection. *Journal of Physical Oceanography*, *25*(5), 855–872. https://doi.org/10.1175/1520-0485(1995)025<0855:ieodc>2.0.co;2

Straneo, F., Pickart, R. S., & Lavender, K. (2003). Spreading of Labrador Sea water: An advective-diffusive study based on Lagrangian data. *Deep Sea Research Part I: Oceanographic Research Papers*, *50*(6), 701–719. https://doi.org/10.1016/s0967-0637(03)00057-8

Tagklis, F., Bracco, A., Ito, T., & Castelao, R. M. (2020). Submesoscale modulation of deep water formation in the Labrador Sea. *Scientific Reports*, *10*(1), 1–13. https://doi.org/10.1038/s41598-020-74345-w

van Aken, H. M., de Jong, M. F., & Yashayaev, I. (2011). Decadal and multi-decadal variability of Labrador Sea water in the north-western North Atlantic Ocean derived from tracer distributions: Heat budget, ventilation, and advection. *Deep Sea Research Part I: Oceanographic Research Papers*, *58*(5), 505–523. https://doi.org/10.1016/j.dsr.2011.02.008

Yan, X., Zhang, R., & Knutson, T. R. (2019). A multivariate AMV index and associated discrepancies between observed and CMIP5 externally forced AMV. *Geophysical Research Letters*, *46*(8), 4421–4431. https://doi.org/10.1029/2019gl082787

Yashayaev, I., & Loder, J. W. (2016). Recurrent replenishment of Labrador Sea water and associated decadal-scale variability. *Journal of Geophysical Research: Oceans*, *121*(11), 8095–8114. https://doi.org/10.1002/2016jc012046

Zanna, L., Khatiwala, S., Gregory, J. M., Ison, J., & Heimbach, P. (2019). Global reconstruction of historical ocean heat storage and transport. *Proceedings of the National Academy of Sciences*, *116*(4), 1126–1131. https://doi.org/10.1073/pnas.1808838115

Zhang, R. (2008). Coherent surface-subsurface fingerprint of the Atlantic meridional overturning circulation. *Geophysical Research Letters*, *35*(20), L20705. https://doi.org/10.1029/2008gl035463

Zhang, R. (2015). Mechanisms for low-frequency variability of summer arctic sea ice extent. *Proceedings of the National Academy of Sciences*, *112*(15), 4570–4575. https://doi.org/10.1073/pnas.1422296112

Zhang, R. (2017). On the persistence and coherence of subpolar sea surface temperature and salinity anomalies associated with the Atlantic multidecadal variability. *Geophysical Research Letters*, *44*(15), 7865–7875. https://doi.org/10.1002/2017gl074342

Zhang, R., Sutton, R., Danabasoglu, G., Kwon, Y.-O., Marsh, R., Yeager, S. G., et al. (2019). A review of the role of the Atlantic meridional overturning circulation in Atlantic multidecadal variability and associated climate impacts. *Reviews of Geophysics*, *57*(2), 316–375. https://doi.org/10.1029/2019rg000644

Zhang, R., & Thomas, M. (2021). Horizontal circulation across density surfaces contributes substantially to the long-term mean northern Atlantic meridional overturning circulation. *Communications Earth & Environment*, *2*(1), 1–12. https://doi.org/10.1038/s43247-021-00182-y

Zou, S. J., & Lozier, M. S. (2016). Breaking the linkage between Labrador Sea water production and its advective export to the subtropical gyre. *Journal of Physical Oceanography*, *46*(7), 2169–2182. https://doi.org/10.1175/JPO-D-15-0210.1

References From the Supporting Information

Ebisuzaki, W. (1997). A method to estimate the statistical significance of a correlation when the data are serially correlated. *Journal of Climate*, *10*(9), 2147–2153. https://doi.org/10.1175/1520-0442(1997)010<2147:amtets>2.0.co;2

Key, R. M., Olsen, A., van Heuven, S., Lauvset, S. K., Velo, A., Lin, X., et al. (2015). Global ocean data analysis project, version 2 (GLODAPv2). *Ornl/Cdiac-162, Ndp-093*.

McDougall, T. J. (1987). Neutral surfaces. *Journal of Physical Oceanography*, *17*(11), 1950–1964. https://doi.org/10.1175/1520-0485(1987)017<1950:ns>2.0.co;2

Thomas, M. D. (2012). Sverdrup balance and three dimensional variability of the meridional overturning circulation PhD thesis. *University of East Anglia*.